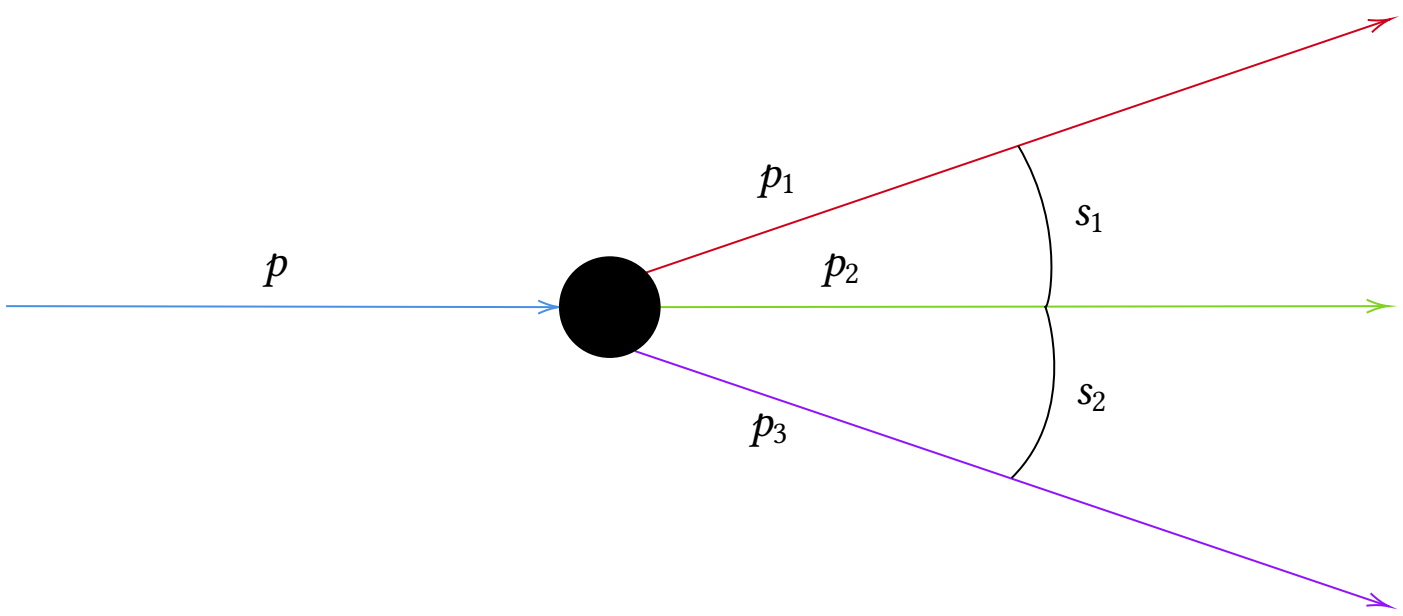


# KINEMATIC INVARIANTS TO ILLUMINATE 3 PARTICLE DECAYS

Martin Mikkelsen

201706771



Bachelor's project  
Supervisors: Karsten Riisager and Hans Fynbo

Department of Physics and Astronomy  
Aarhus University  
Denmark

June 2020



## **Summary**

This is a bachelor's project about relativistic kinematics. This means a theoretical description of particle's motion without considering the forces that cause them to move, in the relativistic limit. More specifically this project illuminates three-particle decays with kinematic invariant quantities. The theory introduces an approach to examine an anomaly that occurred in an experiment when a Hungarian research team measured transitions in  ${}^8\text{Be}$ . It combines considerations of phase space for three-particle decay with resonance amplitudes and angular distributions. This leads to experimental predictions separated into three parts depending on the spin state of the resonant particle, the X17 particle. This project concludes that the formalism is consistent with the relativistic scattering angles in the laboratory system and how experimental results can be illustrated using kinematic invariants. Three angles are proposed to investigate the X17 particle experimentally.

## **Resumé**

Dette bachelorprojekt omhandler relativistisk kinematisk. Det vil altså sige en teoretisk beskrivelse af partiklers bevægelse uden ydre påvirkning i den relativistiske grænse. Mere specifikt belyser dette projekt 3-partikel henfald ved hjælp af kinematiske invariante størrelser. Teorien i projektet introducerer den tilgang, der er anvendt til at undersøge en anormalitet i et forsøg, som opstod da et ungarnsk forskerhold målte overgange i  ${}^8\text{Be}$ . Teorien kombinerer overvejelser omkring faserum for tre-partikel henfald med resonansamplituder og vinkelfordelinger. Dette fører til eksperimentelle forudsigelser, der er inddelt i tre dele afhængig af spintilstanden for resonanspartiklen, X17. Projektet konkluderer, at formalismen er konsistent med den relativistiske spredningsvinkel i laboratoriets hvileramme og viser hvordan eksperimentelle resultater kan repræsenteres ved kinematiske invariante størrelser. Der foreslås tre vinkler, som kan måles eksperimentelt for at undersøge X17 partiklen.

## **Colophon**

*Kinematic invariants to illuminate 3 particle decays*

Bachelor's project by Martin Mikkelsen

The project is supervised by Karsten Riisager and Hans Otto Uldall Fynbo

Typeset by the author using L<sup>A</sup>T<sub>E</sub>X and the memoir document class. Figures are made with the linspecer function in MATLAB

Code can be found on <https://github.com/Martin-Mikkelsen>

Printed at Aarhus University

# Contents

---

<b>Summary / Resumé</b>	<b>2</b>
<b>Preface</b>	<b>5</b>
<b>1 Introduction</b>	<b>6</b>
<b>2 Theory</b>	<b>7</b>
2.1 Notation on Special Relativity . . . . .	7
Energy and Momentum . . . . .	8
2.2 Two-Particle Final States . . . . .	8
Two-Body Decay . . . . .	8
Scattering . . . . .	9
2.3 Three-Particle Final States . . . . .	11
Equal masses . . . . .	11
Non-equal masses . . . . .	14
2.4 Interpretation of the Dalitz Plot . . . . .	17
Resonances . . . . .	20
<b>3 X17</b>	<b>24</b>
3.1 Spin 0 . . . . .	26
3.2 Spin 1 . . . . .	26
3.3 Spin 2 . . . . .	28
<b>4 Discussion</b>	<b>30</b>
<b>5 Conclusion</b>	<b>31</b>
<b>Bibliography</b>	<b>32</b>
<b>Appendix A</b>	<b>34</b>

# Preface

---

This project is a theoretical treatment of relativistic kinematics. More specifically the kinematics concerning decays with three particles in the final state. To illustrate three-body decays I introduce the term kinematic invariants and show how these can be related to a phase-space. In other words, a graphical representation of relativistic kinematics and how one can deduce information about the kinematics. This is called the Dalitz formalism. I will also cover how resonances and spin states are included in this formalism. This can be considered a prerequisite for understanding my approach to analysing the hypothetical X17 particle. I have included a brief section concerning the notation of special relativity I have used and all of the principles should be understood beforehand.

Concerning my choice of subject matter, I was intrigued by the mystery of the X17 particle which is not consistent with the Standard Model of particle physics. Besides that I wanted a better understanding of the special theory of relativity and wanted to combine this with my understanding of general relativity, I have gained in the course Advanced Cosmology. A crossover between cosmology and the X17 particle is outlined in appendix A.

# 1 Introduction

---

The four known forces of nature, the electromagnetic, weak, strong, and gravitational interactions are mediated by the photon, the  $W^\pm$  and  $Z^0$  bosons, the gluon, and the graviton, respectively. This project makes considerations of a particle, the X17, that is hypothesized to carry a fifth force [Feng et al. 2017]. When investigating the transitions in  ${}^8\text{Be}$  Krasznahorkay and his group observed a  $6.8\sigma$  anomaly in the opening angle as a function of the invariant mass of an electron-positron pair [Krasznahorkay et al. 2016]. To explain this anomaly theorists hypothesized a 17 MeV particle. This particle was produced in the decay of an excited state in beryllium to its ground state, that is  ${}^8\text{Be}^* \rightarrow {}^8\text{Be} + X$ , where  $X$  is the 17 MeV particle and hence the name X17. This particle then decays into an electron-positron pair,  $X \rightarrow e^- + e^+$ . If the electron-positron pair was produced by the photon, the scattering angle would be close to  $0^\circ$  – due to conservation of momentum. They measured a scattering angle of  $140^\circ$  and the data did not suggest a photon.

The group then searched for new evidence supporting the hypothetical X17 boson by measuring the electron-positron pair produced in the electromagnetically forbidden M0 transition in  ${}^4\text{He}$ . A peak in the positron-electron angular correlation was found at  $115^\circ$  with  $7.2\sigma$  significance. This could be explained by the creation and subsequent decay of a particle with mass,  $m_X c^2 = 16.84 \pm 0.16(\text{stat.}) \pm 0.20(\text{syst.})$ . This is consistent with the particle mass hypothesised in the beryllium experiment.

The theory of the X17 boson gained traction when Jonathan Feng et al. made theoretical considerations of the particle and concluded that a 17 MeV vector gauge boson could explain the anomaly observed in the  ${}^8\text{Be}$  decay [Feng et al. 2016]. They concluded that the new particle could mediate a fifth force with a characteristic length scale of 12 fm. The considerations they made are outlined in appendix A.

In this project, I will make an approach through relativistic kinematics and look at the constraints one can make from this formalism and how the experimental results can be represented. More specifically I will consider the decay  ${}^4\text{He}^* \rightarrow {}^4\text{He} + e^+ + e^-$  as a three-particle decay and see what constraints and possibilities this gives rise to.

# 2 Theory

---

In the following section, I will describe relativistic particle kinematics in different scenarios. Firstly, I will define the notation for special relativity then I will define the mathematical expressions I have used in the following sections. I start by considering the decay processes with two particles in the final state and will also derive an expression for the energy in the centre of mass frame. I also cover  $2 \rightarrow 2$  scattering and introduce the Mandelstam variables.

This leads to processes with three particles in the final state and I will show the basics of Dalitz plot. I have split this into two sections; one for equal masses in the final state to highlight symmetry arguments and also a general case. Lastly, I will go through an interpretation of the Dalitz plot formalism. Specifically, I will cover how regions in the plot are connected to momentum configurations and how resonances will appear in the plot.

## 2.1 Notation on Special Relativity

I will be using the following notation for four-vectors. In a 4-dimensional Minkowski space, the position-time four-vector is given by [Uggerhøj 2016, 198]

$$x \equiv (x^0, x^1, x^2, x^3) = (ct, \mathbf{x}). \quad (2.1)$$

The Lorenz transformations are linear transformations on four-vectors and the scalar product is invariant. A quantity is invariant when it has the same value after some particular transformation. A quantity is conserved when it takes the same value before and after a particular event. In a collision between particles, the four-momentum is conserved within a particular frame of reference but not invariant between frames. [Lancaster and Blundell 2014]. This motivates the use of invariant quantities.

Transformations from one frame to another frame with velocity  $v_x$  along the  $x$ -axis is given by

$$\Lambda = \begin{pmatrix} \gamma & -\beta\gamma & 0 & 0 \\ -\beta\gamma & \gamma & 0 & 0 \\ 0 & 0 & 1 & 0 \\ 0 & 0 & 0 & 1 \end{pmatrix}, \quad \gamma = \frac{1}{\sqrt{1-\beta^2}}, \quad \beta = \frac{v}{c}. \quad (2.2)$$

In equation (2.2) the speed of light,  $c$ , appears explicitly. In the rest of the project I will be using natural units that is  $\hbar = c = k_B = 1$ .

## Energy and Momentum

I will be using the following useful relations for the boost factor,  $\gamma$  and the velocity of a particle  $\beta$  [Zyla and others Particle Data Group, 1]

$$\gamma = \frac{E}{m}, \quad \beta = \frac{\mathbf{p}}{E}. \quad (2.3)$$

It is also convenient to introduce the triangle function [Martin and Shaw 2019, 462]

$$\lambda(x, y, z) \equiv (x - y - z)^2 - 4xyz. \quad (2.4)$$

This function is invariant under all permutations of its arguments.

## 2.2 Two-Particle Final States

In this section I consider the simplest kinematical process – one particle going into two particles. This section should be considered an introduction to working with 4-momenta related to decay and scattering.

### Two-Body Decay

Consider a particle of mass  $M$  decaying into two particles with masses  $m_1$  and  $m_2$  i.e. a process on the form  $M \rightarrow m_1 + m_2$  in the centre of mass frame. In special relativity a better name would be centre of momentum since the CM frame is defined by  $\mathbf{P} = \sum \mathbf{p} = 0$ . Using invariant four-vector products the energies  $E_1$  and  $E_2$  are calculated in the centre of momenta system

$$p_1^2 = p^2 + p_2^2 - 2p \cdot p_2, \quad (2.5)$$

$$m_1^2 = M^2 + m_2^2 - 2ME_2. \quad (2.6)$$

The energy of particle 2,  $E_2$  is then given by

$$E_2 = \frac{M^2 - m_1^2 + m_2^2}{2M} \quad (2.7)$$

Similarly for the energy of particle 1

$$p_2^2 = p^2 + p_1^2 - 2p \cdot p_1, \quad (2.8)$$

$$m_2^2 = M^2 + m_1^2 - 2ME_1. \quad (2.9)$$

The energy of particle 1 in the CMS is

$$E_1 = \frac{M^2 + m_1^2 - m_2^2}{2M} \quad (2.10)$$

The centre of momenta system, called the CMS from now on, is given by

$$|\mathbf{p}_1| = |\mathbf{p}_2| = \frac{[(M^2 - (m_1 + m_2)^2)(M^2 - (m_1 - m_2)^2)]^{\frac{1}{2}}}{2M}. \quad (2.11)$$

Equation (2.11) shows that a decay is only possible when  $M > m_1 + m_2$ . The threshold value  $m_1 + m_2$  is the smallest value for  $M$ . It is possible to relate this to the velocity of the particles  $m_1$  and  $m_2$  [Byckling and Kajantie 1973, 24]. The smallest value occurs when  $|\mathbf{v}_1| = |\mathbf{v}_2|$ . This will be justified in section 2.4 but I want to emphasize that considerations of the velocity of the particles in the CMS is of great use for decay processes.

## Scattering

In the following, I will be considering the invariant variables for  $2 \rightarrow 2$  scattering. Using kinematic invariants is a fundamental part of this project and in this section, I consider invariants for the process

$$p_a + p_b \rightarrow p_1 + p_2. \quad (2.12)$$

Using the Mandelstam variables defined by [Martin and Shaw 2019, 463]

$$s \equiv (p_a + p_b)^2 = (p_1 + p_2)^2 \quad (2.13)$$

$$t \equiv (p_a - p_1)^2 = (p_b - p_2)^2 \quad (2.14)$$

$$u \equiv (p_a - p_2)^2 = (p_b - p_1)^2, \quad (2.15)$$

where  $p_a$  and  $p_b$  are the four-momenta of the two incoming particles and  $p_1$  and  $p_2$  are the four-momenta of the outgoing particles. Equation (2.13) is also called the square of the centre of mass energy and equation (2.14) is called the square of four-momentum transfer. Equation (2.15) is related to crossing. The Mandelstam variables are illustrated in figure 2.1 a)

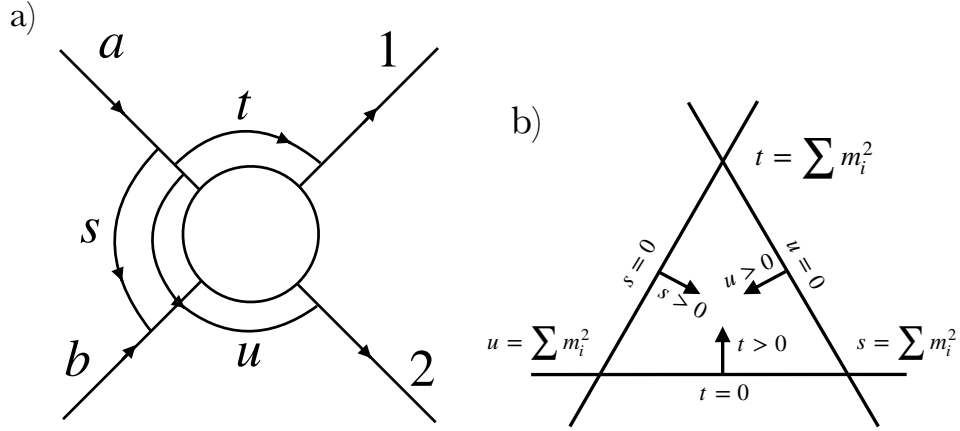


Figure 2.1: a) Illustration of the invariant variables for  $p_a + p_b \rightarrow p_1 + p_2$ . b) Triangular coordinates for  $s, t, u$ .

The Mandelstam variables are related by a linear relation

$$s + t + u = p_a^2 + p_b^2 + p_1^2 + (p_a + p_b - p_1)^2 \quad (2.16)$$

$$= m_a^2 + m_b^2 + m_1^2 + m_2^2. \quad (2.17)$$

I show this equation to empathize how the masses and kinematic invariants constrain each other. The Mandelstam variables are convenient since they relate the energy, momentum and scattering angle to the masses of the particles in an invariant manner. I will not be going through this in this project since I will focus on 3-particle decays and here the Mandelstam variables also play an important role.

For instance if  $m_b > m_a + m_1 + m_2$  the following decay is possible

$$p_b \rightarrow p_{\bar{a}} + p_1 + p_2, \quad (2.18)$$

where the bar denotes antiparticle. This is important because this relates a particle with 4-momentum  $p$  to its antiparticle with 4-momentum  $-p$ . For instance the emission of a positron and the absorbtion of an electron. This is effectively a three-particle decay since there are three particles in the final state.

In this section, I have outlined the approach of treating two-particles in the final state. I have done this to pave the way for treating three particles in the final state. They have the same number of invariants<sup>1</sup> and are related by the crossing, equation (2.15). This is the bridge between  $2 \rightarrow 2$  and  $1 \rightarrow 3$  processes.

---

<sup>1</sup>The particles are spinless.

## 2.3 Three-Particle Final States

In the following, I will be considering processes in which the final state consists of three particles. I will be showing a visual representation of the kinematic properties of a three-body decay for spinless particles. This is also known as a Dalitz plot. I will derive expressions for the boundary curve due to conservation of momentum. This means any event outside this boundary is not physically possible. I have split this into two different cases. One where the masses in the final state are equal because this illustrates how one can use symmetry arguments to get an expression for the boundary curve. After this, I will generalize the boundary curve to different masses in the final state and show the result on a plot consisting of two axes of invariant masses.

### Equal masses

I will outline an approach to the boundary curve in the specific case where all the masses in the final state are equal. The boundary curve is a region where all events must lie within due to conservation of momentum. The main idea is to exploit the symmetry and plot in triangular coordinates where the enclosed area is available from energy conservation. Then imply a restriction on what regions are allowed due to conservation of momentum. This restriction is found by starting in the centre of the triangle where the energies of the particles in the final state must be the same and then introduce an angle and a distance to all other points. This will ultimately lead to a boundary curve which is dependent on the relativistic limit. The following is inspired by [Hagedorn 1963, 103]

I will make use of the three Mandelstam variables mentioned in section 2.1 since these three variables can be plotted in a plane where they represent the distances from three sides of a triangle. The three lines are the axes intersecting at  $60^\circ$  and the Mandelstam variables  $s, t, u$  are the distances from the corresponding axes. This is illustrated on figure 2.1 b). In the case with equal masses I make use of equation (2.17) which means  $s + t + u = 4m^2$ . This condition is fulfilled when the height of the triangle between the lines is  $\sum m_i^2$  [Byckling and Kajantie 1973, 93].

In this specific case the decay is given by

$$M \rightarrow m_1 + m_2 + m_3, \quad (2.19)$$

where the masses are equal  $m_1 = m_2 = m_3 = m$  and are related to the mass of the decaying particle by [Hagedorn 1963, 100]

$$T_1 + T_2 + T_3 = M - 3m = Q, \quad (2.20)$$

where  $Q$  is the total kinetic energy. It is convenient to make the symmetry explicit by using all three energies. An equilateral triangle of height  $Q$  is introduced ad hoc. If all the particles in the final state have the same kinetic energy, this can be represented as the centre of the triangle – i.e.  $T_1 = T_2 = T_3 = Q/3$ .

For all other events inside the triangle the distance,  $\rho$  and the angle  $\phi$  is introduced. This is illustrated in figure 2.2. These quantities are related to the kinetic energies in the following way

$$T_1 = \frac{Q}{3} (1 + \rho \cos(\phi_1)), \quad \phi_1 = \phi - \frac{2\pi}{3} \quad (2.21)$$

$$T_2 = \frac{Q}{3} (1 + \rho \cos(\phi_2)), \quad \phi_2 = \phi + \frac{2\pi}{3} \quad (2.22)$$

$$T_3 = \frac{Q}{3} (1 + \rho \cos(\phi_3)), \quad \phi_3 = \phi, \text{ angle in figure 2.2.} \quad (2.23)$$

It is now possible to determine the boundary curve, that is, a curve that defines a region where all events must lie within due to the restriction from conservation of momentum. From conservation of momentum

$$(\mathbf{p}_1 + \mathbf{p}_2)^2 = \mathbf{p}_3^2, \quad (2.24)$$

which is expanded and rewritten using  $p_i = |\mathbf{p}_i|$

$$(p_1 + p_2)^2 = p_1^2 + p_2^2 + 2p_1 p_2 \cos \theta = p_3^2, \quad (2.25)$$

where  $\theta$  is the angle between  $p_1$  and  $p_2$ . The cosine of this angle goes from 1 to -1. This leads to

$$4p_1 p_2 \geq (p_3^2 - p_1^2 - p_2^2)^2, \quad (2.26)$$

where the equality must mean maximum and can therefore be interpreted as the boundary curve. The boundary curve is then defined by  $\cos \theta = \pm 1$ . I express the momenta in terms of the kinetic energies and use the following relation

$$p_i^2 = E_i^2 - m_i^2 = T_i + 2m_i T_i. \quad (2.27)$$

There is no index on the mass term in the last equality because the masses in the final state are equal, that is, equation (2.20). This leads to

$$T_1^2 + T_2^2 + T_3^2 = \frac{Q^2}{9} \left( 3 + 2\rho \underbrace{(\cos \phi_1 + \cos \phi_2 + \cos \phi_3)}_{=0} + \rho^2 \underbrace{(\cos^2 \phi_1 + \cos^2 \phi_2 + \cos^2 \phi_3)}_{=3/2} \right) \quad (2.28)$$

where I have used that the total energy is  $T_1 + T_2 + T_3 = Q$  which means  $\cos \phi_1 + \cos \phi_2 + \cos \phi_3 = 0$ . This yields

$$\sum_i^3 T_i = Q, \quad \sum_i^3 T_i^2 = \frac{Q^2}{3} \left( 1 + \frac{1}{2} \rho^2 \right). \quad (2.29)$$

This can be rewritten using many different steps. A final expression for the distance squared,  $\rho^2$  remains. This means any event on the triangle must lie within the boundary curves defined by

$$\rho^2 = \frac{1}{1 + \frac{2\sigma}{(2-\sigma)^2}(1 + \rho \cos 3\phi)}, \quad \sigma = \frac{Q}{M} \quad (2.30)$$

To justify this expression I consider different limits. I consider the ultra-relativistic limit ( $\sigma = 1$ ) and the non-relativistic limit ( $\sigma = 0$ ). Also an event cannot lie in the corner of the triangle since this would imply that only one of the particles are moving while the two others are at rest which is not allowed from  $\mathbf{p}_1 + \mathbf{p}_2 + \mathbf{p}_3 = 0$ . Also, note that  $\rho$  appears on both sides of the equation.

$$\rho^2 : \begin{cases} 1 & \sigma = 0, \text{ non-relativistic} \\ \frac{1}{1+2(1+\rho \cos 3\phi)} & \sigma = 1, \text{ ultra-relativistic} \end{cases} \quad (2.31)$$

The interpretation of equation (2.31) is that the non-relativistic limit yields an inscribed circle since we must have  $\phi = \pi$ . Inserting this into equation (2.21), equation (2.22) and equation (2.23) shows the circle touches the sides of the triangle.

The ultra-relativistic limit is found by rewriting the ultra-relativistic case of equation (2.31) to  $2\rho^3 \cos 3\phi + 3\rho^2 - 1 = 0$  and identifying the solution as  $\rho \cos \phi = 1/2$  which represents a vertical side of the inscribed triangle. The two other lines follow from symmetry.

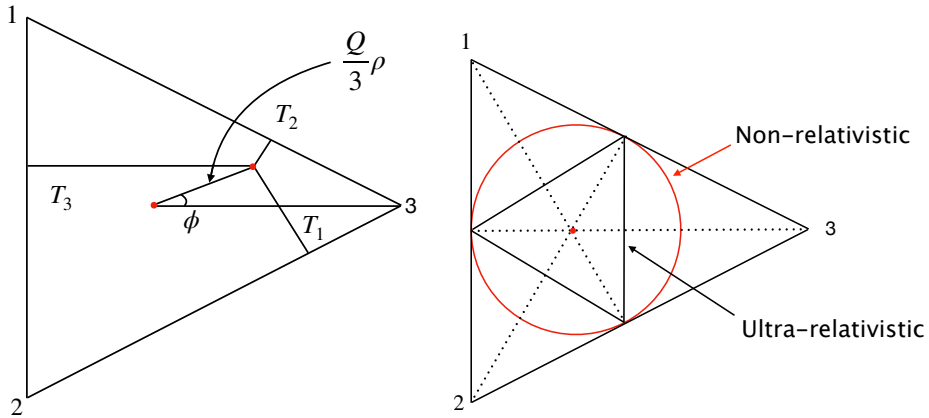


Figure 2.2: Dalitz plot for equal masses. The figure on the left hand side shows the kinetic energies and the angle  $\phi$ . The arrow with  $Q\rho/3$  is pointing to the line between the two red dots. The figure on the right hand side shows the boundary curve in the non-relativistic and ultra-relativistic limit.

In conclusion, I have defined a region with restrictions due to energy conservation and conservation of momentum. This means events must be within these regions. The shape of boundary curve changes in different relativistic limits and this can be expressed mathematically as  $0 < \sigma < 1$ . This is illustrated in figure 2.2.

## Non-equal masses

In the case of non-equal masses, a few more definitions are required. I will start by defining a new set of invariant variables analogues to equation (2.13). The invariant variables are defined as

$$s_{12} \equiv s_1 = (p_1 + p_2)^2 = m_1^2 + m_2^2 + E_1 E_2 - \mathbf{p}_1 \cdot \mathbf{p}_2 = m_{12}^2 \quad (2.32)$$

$$s_{23} \equiv s_2 = (p_2 + p_3)^2 = m_2^2 + m_3^2 + E_2 E_3 - \mathbf{p}_2 \cdot \mathbf{p}_3 = m_{23}^2 \quad (2.33)$$

$$s_{31} \equiv s_3 = (p_3 + p_1)^2 = m_3^2 + m_1^2 + E_3 E_1 - \mathbf{p}_3 \cdot \mathbf{p}_1 = m_{31}^2, \quad (2.34)$$

These equations show what notation I will be using throughout the text. I will be switching between  $s_i$  and  $m_{ij}^2$  primarily. When I refer to an invariant mass, I refer to these equations.

The equations above are related in the following way similar to equation (2.17)

$$s_1 + s_2 + s_3 = s + m_1^2 + m_2^2 + m_3^2 = \text{constant}, \quad s = M^2 \quad (2.35)$$

where  $M$  is the mass of the decaying particle. I will now express the energy and momentum of the particles in terms of these invariant variables. This will ultimately lead to how the energies and momenta of the particles are restricted.

To express the energy and momentum in terms of the invariant variables a consideration of the rest frames is needed. There are three possible rest frames corresponding to the Mandelstam variables in  $2 \rightarrow 2$  scattering. The three-particle decay  $p \rightarrow p_1 + p_2 + p_3$  is related by crossing to  $2 \rightarrow 2$  scattering,  $p + p_{\bar{1}} \rightarrow p_2 + p_3$  and the number of invariants must be the same. The three possible rest frames corresponds to the  $s, t, u$  channels in  $2 \rightarrow 2$  scattering and are giving by

$$\mathbf{p}_1 + \mathbf{p}_2 = \mathbf{p} - \mathbf{p}_3 = 0 \quad (2.36)$$

$$\mathbf{p}_2 + \mathbf{p}_3 = \mathbf{p} - \mathbf{p}_1 = 0 \quad (2.37)$$

$$\mathbf{p}_3 + \mathbf{p}_1 = \mathbf{p} - \mathbf{p}_2 = 0. \quad (2.38)$$

These frames are called the Gottfried-Jackson frames and quantites in these frames are denoted by the superscript  $Rij$  – the R stands for rest. It is sufficient to consider one of these frames,  $R23$ , since equations relating the energy and

momentum to the other frames are related by cyclic permutation of the indices [Byckling and Kajantie 1973, 105]. The rest frame of the system formed by  $\mathbf{p}_2 + \mathbf{p}_3 = \mathbf{0}$  is illustrated in figure 2.3.

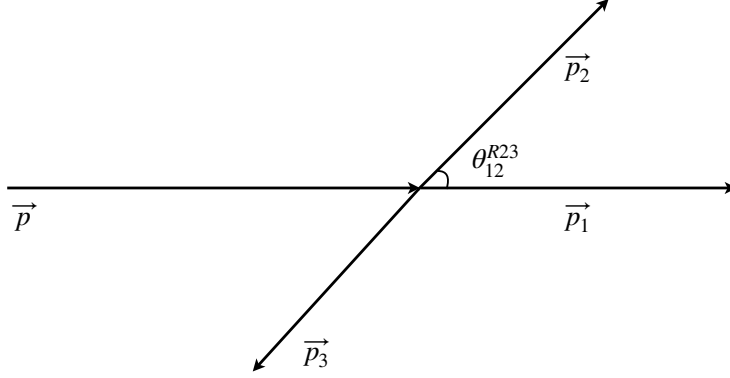


Figure 2.3: Three-particle decay in the rest frame of the system formed by the particles 2 and 3. That is  $\mathbf{p}_2 + \mathbf{p}_3 = \mathbf{0}$ . Note the similarity to  $2 \rightarrow 2$  scattering mentioned in section 2.2. See figure 2.1.

I have expanded equation (2.32) to illustrate how one can derive expressions for the energy and momentum. The energies and momenta in the frame  $\mathbf{p}_2 + \mathbf{p}_3 = \mathbf{0}$  can be expressed in terms of invariants

$$E_1^{R23} = \frac{s - s_2 - m_1^2}{2\sqrt{s_2}}, \quad (2.39)$$

$$E_2^{R23} = \frac{s_2 + m_2^2 - m_3^2}{2\sqrt{s_2}}, \quad (2.40)$$

$$P_1^{R23} = \frac{\lambda^{\frac{1}{2}}(s, s_2, m_1^2)}{2\sqrt{s_2}}, \quad (2.41)$$

$$P_2^{R23} = \frac{\lambda^{\frac{1}{2}}(s_2, m_2^2, m_3^2)}{2\sqrt{s_2}}. \quad (2.42)$$

These are inserted into equation (2.32)

$$s_1 = (p_1 + p_2)^2 \quad (2.43)$$

$$= m_1^2 + m_2^2 + 2E_1^{R23}E_2^{R23} - 2P_1^{R23}P_2^{R23} \cos(\theta_{12}^{R23}) \quad (2.44)$$

$$= m_1^2 + m_2^2 + \frac{1}{2s_2} \left[ (s - s_2 - m_1^2)(s_2 + m_2^2 - m_3^2) - \cos(\theta_{12}^{R23}) \lambda^{\frac{1}{2}}(s_1, s_2, m_1^2) \lambda^{\frac{1}{2}}(s_2, m_2^2, m_3^2) \right] \quad (2.45)$$

This can be rewritten assuming  $\cos(\theta_{12}^{R23}) = \pm 1$  which yields  $s_1$  as a function of  $s_2$ . This is equivalent to the assumption I made in equation (2.26) where the

maximum must represent a boundary. This assumption will be justified in section 2.4. Equation (2.45) defines a boundary curve on a  $s_1, s_2$  plot analogous to equation (2.30) in the case of equal masses. The  $\pm$  refers to the upper and lower half of the boundary curve respectively.

$$s_1^\pm = m_1^2 + m_2^2 - \frac{1}{2s_2} \left[ (s_2 - s + m_1^2)(s_2 + m_2^2 - m_3^2) \mp \lambda^{\frac{1}{2}}(s_1, s_2, m_1^2) \lambda^{\frac{1}{2}}(s_2, m_2^2, m_3^2) \right] \quad (2.46)$$

This is the final equation which defines the boundary curve for three particles in the final state. The equation describing  $s_2$  as a function of  $s_1$  represents the same boundary curve but with different numerical advantages.

One example of a Dalitz plot can be seen on figure 2.4. I have chosen the decay  $D_s^+ \rightarrow \pi^+ + \pi^- + \pi^-$  to show how the Dalitz plot is symmetric for equal masses. This can be compared to the symmetric case in figure 2.2 and the non-symmetrical case in figure 2.5.

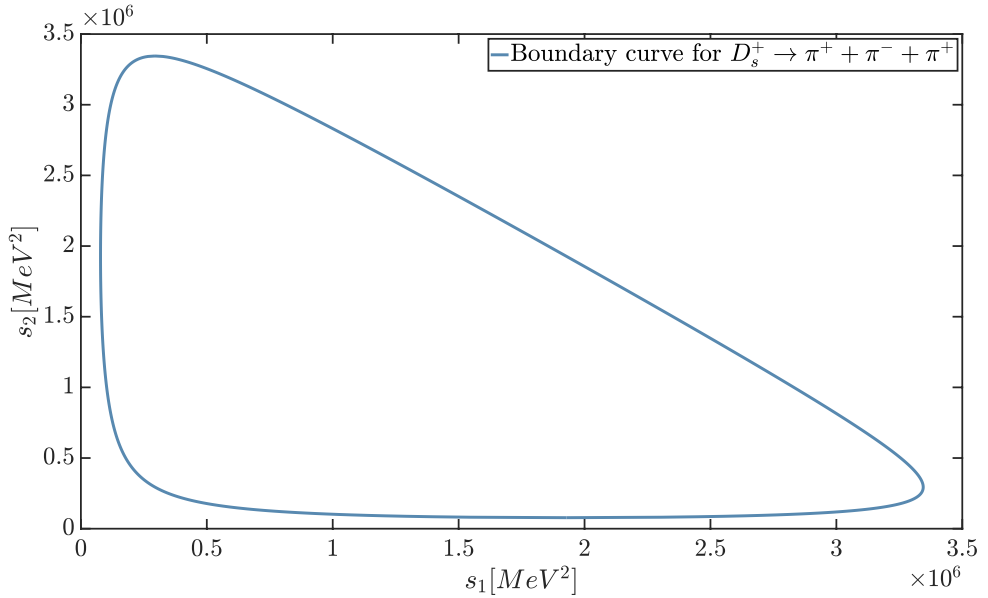


Figure 2.4: Dalitz plot for  $D_s^+ \rightarrow \pi^+ + \pi^- + \pi^-$ . The Dalitz plot defines a boundary curve due to conservation of momentum. Any event outside the boundary is not possible.

Equation (2.45) can also be used to get an analytical expression for the angle between particle 1 and particle 2 in the rest frame of 2 and 3 which is given by

$$\cos \theta_{12}^{R23} = \frac{(s - s_2 - m_1^2)(s_2 + m_2^2 - m_3^2) + 2s_2(m_1^2 + m_2^2)}{\lambda^{\frac{1}{2}}(s, s_2, m_1^2)\lambda^{\frac{1}{2}}(s_2, m_2^2, m_3^2)} \quad (2.47)$$

Equation (2.47) shows that the angular correlation between the particles in the final state change as a function of  $s_2$ . This means different momentum configurations correspond to different regions and this will be covered in the next section.

## 2.4 Interpretation of the Dalitz Plot

In the previous section, I outlined an analytical approach to the boundary curve on a  $s_1, s_2$  plot. In this section, I wish to illustrate how one can interpret the Dalitz plot. I will be covering what the different regions in the plot represent physically and how resonances manifest themselves as intensity variations within the boundary curve.

Consider equations (2.32), (2.33) and (2.34) and the energies in the rest frame of  $M$ , that is the decaying particle. In this rest frame, the momenta of the particles lie in a plane and the relative orientation is fixed. By introducing three Euler angles  $(\alpha, \beta, \gamma)$  one can specify the orientation of the final system relative to the initial particle.

This can be combined with the transition rate  $d\Gamma$  from perturbation theory of spinless particles given by [Zyla and others Particle Data Group, 4]

$$d\Gamma = \frac{(2\pi)^4}{2M} |\mathcal{M}|^2 \delta^4 \left( P - \sum_{i=1}^3 p_i \right) \prod_{i=1}^3 \frac{d^3 p_i}{(2\pi)^3 2E_i}, \quad (2.48)$$

which in terms of the energies and the Euler angles yields

$$d\Gamma = \frac{1}{(2\pi)^5} \frac{1}{16M} |\mathcal{M}|^2 dE_1 dE_2 d\alpha d(\cos \beta) d\gamma. \quad (2.49)$$

Integrating over the angles gives

$$d\Gamma = \frac{1}{(2\pi)^3} \frac{1}{8M} \overline{|\mathcal{M}|^2} dE_1 dE_2, \quad (2.50)$$

which rewritten in terms of the masses is

$$d\Gamma = \frac{1}{(2\pi)^3} \frac{1}{32M^3} \overline{|\mathcal{M}|^2} dm_{12}^2 dm_{23}^2. \quad (2.51)$$

From equation (2.51) there are two results. The three-body decay can be described by two invariant masses and the square of the matrix element – called the invariant amplitude from now on and denoted by  $\mathcal{A}$ . The result that a three-body decay can be described using two invariant masses can also be justified by considering the degrees of freedom. In a three-body decay, there are 3 four-vectors in the final state. This means there are 12 degrees of freedom. To describe these I make use of conservation of 4-momentum which has 4 degrees of freedom, 3 degrees of freedom from the masses in the final state, and lastly the 3 Euler angles  $\alpha, \beta, \gamma$ . Therefore the total degrees of freedom is 2 which is consistent with equation (2.51).

If the invariant amplitude is constant this region is uniformly populated with events. This also means any deviations from uniformity yields information on  $|\mathcal{A}|^2$ . It is also possible to extract information about the kinematical configurations of the particles from the Dalitz plot and vice versa. I consider the centre of mass frame in which all three momenta vectors sum to zero,  $\mathbf{p}_1 + \mathbf{p}_2 + \mathbf{p}_3 = \mathbf{0}$ . From equation (2.47) one can show that the invariant masses in equation (2.32), (2.33) and (2.34) must satisfy

$$(m_1 + m_2)^2 \leq s_1 \leq (M - m_3)^2 \quad (2.52)$$

$$(m_2 + m_3)^2 \leq s_2 \leq (M - m_1)^2 \quad (2.53)$$

$$(m_1 + m_3)^2 \leq s_3 \leq (M - m_2)^2 \quad (2.54)$$

I will now use these relations to get information about the configuration of particles and how this can be interpreted in the Dalitz plot. I will show this with an example and explain that this can be generalized for all three particles in the final state. The minimum of  $s_1 = (m_1 + m_2)^2$  must be when  $\mathbf{p}_1 \cdot \mathbf{p}_2 = m_1 m_2$  is fulfilled, that is, when the velocities are the same,  $\mathbf{v}_1 = \mathbf{v}_2$  [Byckling and Kajantie 1973, 113]. This is also the condition I mentioned in section 2.2.

What this means physically is that the particles move together as one particle. When this occurs  $E_3$  and  $P_3$  must have a maximum, where these refer to the energy and momentum I used in equation (2.45). This yields one of the coordinates in the Dalitz plot and the other coordinate is found by using equation (2.45). This can be generalized for all three  $s_i, i = 1, 2, 3$ . At the point where  $s_i = s_{ij}^{\min} = (m_i + m_j)^2$  particle  $i$  and  $j$  move in the same direction with equal velocity and particle  $k$  moves in the complete opposite direction with the maximum value of momentum it can attain in the CMS.

Now, considering the maximum  $s_1 = s_1^{\max}$ . This means that  $E_3 = m_3$  and  $P_3 = 0$  – both energy and momentum attain their smallest value in the centre of mass frame. This is the maximum of  $s_1 = (M - m_3)^2$ . Physically this means that particle 3 is at rest and particle 1 and 2 move in opposite directions.

In figure (2.5) I have made a Dalitz plot of the decay  $B_s^0 \rightarrow \bar{D}^0 + K^- + \pi^+$  with minima and maxima of  $s_1$ ,  $s_2$ ,  $s_3$  included as blue and red dots respectively. I have also included the momenta of all particles represented as coloured arrows. I have chosen this specific decay since all the decay products have different masses and the Dalitz plot does not look symmetric.

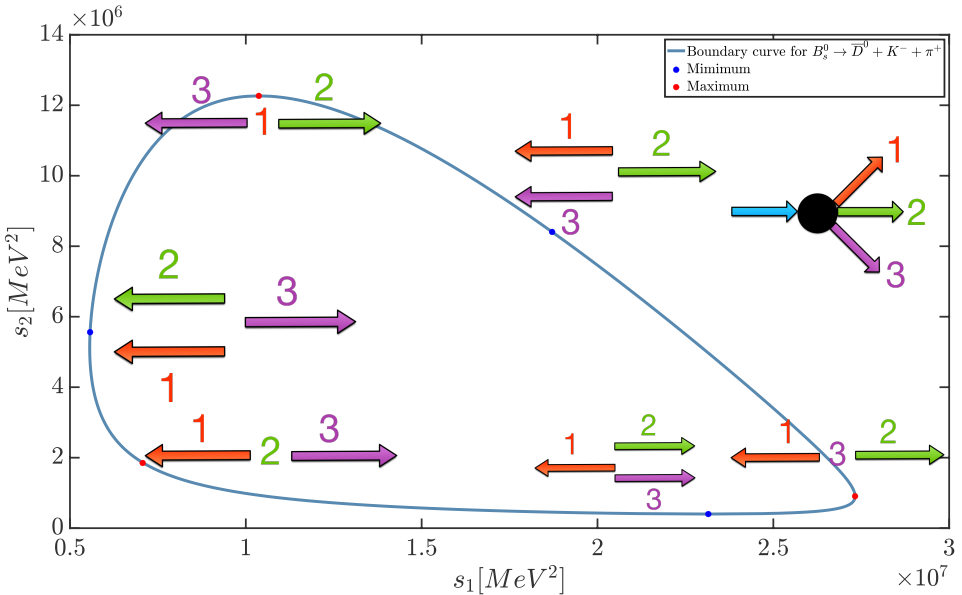


Figure 2.5: The kinematic properties of the Dalitz plot with  $s_2$  as a function of  $s_1$ . I have colour-coded the decay products so particle 1 is the red arrow, particle 2 is green and particle 3 is purple. I have chosen this decay since all the decay products have different masses. This blue curve represents the same boundary curve derived from equation (2.45). The blue and red dots represent the minimum and maximum respectively. The directions of the arrows indicate momentum of the decay products.

In short, the section above has highlighted that it is possible to relate the momentum configurations to specific regions in the Dalitz plot. From this result, it is possible to extract information about the angle between particles in a three-body decay. If the population of events is nonuniformly distributed within the boundary curve one can tell what kinematic configurations occur more often than others. Since a three-body decays can go through an intermediate particle, which subsequently decays, this is related to the resonance state of the intermediate particle.

## Resonances

Resonances are observed not only in atomic and nuclear physics but in also particle physics. In the following, I will explain how resonances of particles manifest themselves in the Dalitz plot.

Resonances lead to sharp and often distinctive peaks in the total cross-section as a function of energy. The sharp variation of the cross-section is related to a nearly bound state of the particle target with a given energy,  $E_R$ . When a particle is sent in with the same energy,  $E_R$ , it can be temporarily captured into this metastable state and this possibility is considered the cause of the variations in the cross-section. In particular, the partial cross-section where the background phase is zero is given by the non-relativistic Breit-Wigner formula [Taylor 1972, 238]

$$\sigma(E) \propto \frac{(\Gamma/2)^2}{(E - E_R)^2 + (\Gamma/2)^2}, \quad \Gamma = \frac{1}{\tau} \quad (2.55)$$

In the case where particles are moving at relativistic velocities the behavior of the resonance can be described by using the relativistic Breit-Wigner amplitude

$$\mathcal{A}_{\text{BW,rel}} \simeq \frac{\sqrt{s_{ab}}}{M_R^2 - s_{ab} - i\Gamma\sqrt{s_{ab}}}, \quad (2.56)$$

where  $s_{ab}$  is the invariant mass of the decay channel  $ab$  and the subscript  $R$  represents an intermediate resonant state that subsequently undergoes a two-body decay. The subsequent decay can be expressed in the following way and is illustrated in figure 2.6

$$A \rightarrow (ab)b, \quad (2.57)$$

where  $(ab)$  is the intermediate resonant state.

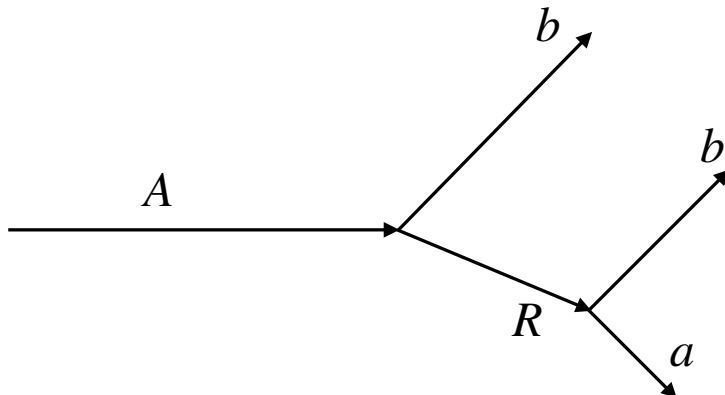


Figure 2.6: shows a decay with an intermediate state,  $R$ . This can be expressed in the following way  $A \rightarrow (ab)b$ , where  $(ab)$  is the intermediate resonant state.

Returning to the Dalitz plot formalism and considering the final state of the process in equation (2.57). The distribution of events along the axis  $s_1$ , in this case, will be more dense in the region near the mass of the resonant state,  $M_R$ .

In general, this can be seen on the Dalitz plot as a band of events along one of the axis. For an example see figure (2.7). The density of events resembles a band that is parallel to one of the coordinate axis or along a  $45^\circ$  line [Martin and Shaw 2019, 463].

The resonant state can occur for any two-body decay channel in the three-body decay corresponding to three possible directions of the band. The two-body decay channels can be shown in the following way

$$A \rightarrow (ab)c, \quad A \rightarrow a(bc), \quad A \rightarrow (ac)b, \quad (2.58)$$

where the pair in the parenthesis is the resonant state.

Since the two-body decay can go through any of the decay channels the resulting Dalitz plot is a superposition of the events. In other words, the density of events along the different axis can interfere constructively and destructively.

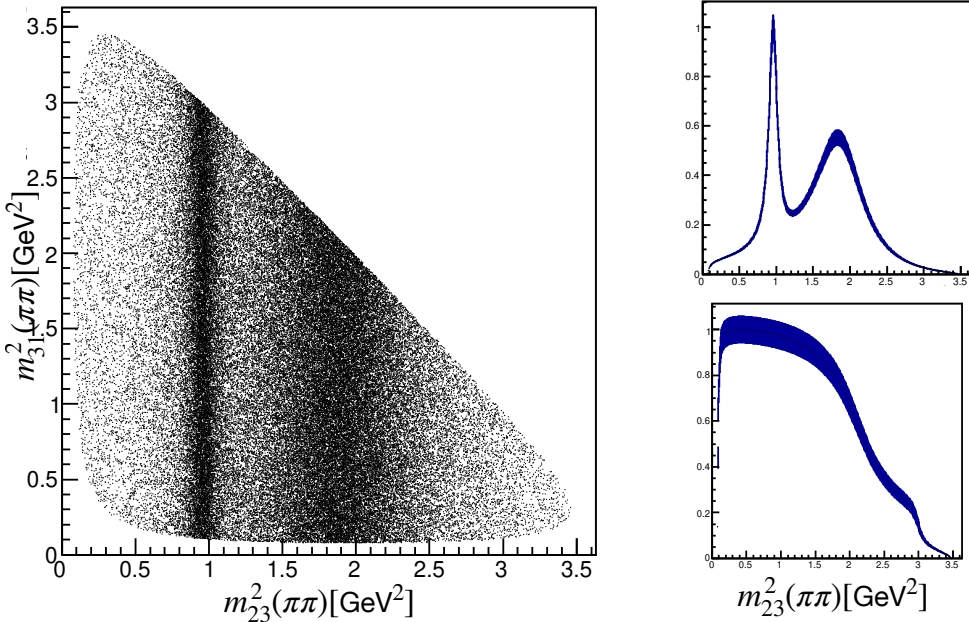


Figure 2.7: Numerical Dalitz plot of a particle with a mass equal to 2 GeV decaying into three pions. The figures of the right-hand side show the projections onto the  $m_{23}^2$  and  $m_{31}^2$  respectively. This plot also shows how the density of events is distributed according to the resonances. This plot is made with a ROOT based tool to illustrate 3-body decays [Goetzen 2014]. The boundary curve is identical to figure 2.4.

In figure 2.7 a numerical procedure of the Dalitz plot of a particle with mass 2 of GeV decaying into 3 pions is illustrated [Goetzen 2014]. Figure 2.7 also includes the following resonances in (23):  $f_0(980)$  and  $f_0(1370)$ . The resonances in (23) are perpendicular to the axis  $m_{23}^2$ . In the projection of  $m_{23}^2$  there is a distinctive peak which is also represented in the Dalitz plot. There is also a smaller, broader peak which also appears in the Dalitz plot.

When taking the spin of the resonant state into account the band is not constant along the axis. For three spinless particles in the final state, the invariant amplitude in equation (2.56) is proportional to Legendre polynomial of order  $l$  where  $l$  is the spin of the resonance [Londergan 2015, 22]. The Legendre polynomial is a function of the angle between the two particles in the resonant state. From the definition of the boundary curve and figure 2.5 this angle goes from 1 to  $-1$ . The invariant amplitude is then given by

$$\mathcal{A} \sim \mathcal{A}_{\text{BW,rel}} P_l(\cos \theta^{Rab}). \quad (2.59)$$

The Legendre polynomials are defined by [Jackson 1999, 99]

$$P_l(x) = \frac{1}{2^l l!} \frac{d^l}{dx^l} (x^2 - 1)^l, \quad (2.60)$$

which for different orders of  $l$  yields

$$P_l(\cos \theta) = \begin{cases} 1, & l = 0 \\ \cos \theta, & l = 1 \\ \frac{1}{2} (3 \cos^2 \theta - 1), & l = 2 \end{cases} \quad (2.61)$$

From this the final expression for the invariant amplitude is

$$|\mathcal{A}|^2 = \left| \mathcal{A}_{\text{BW,rel}} P_l \cos \theta^{Rab} \right|^2 \quad (2.62)$$

I have illustrated the behaviour of the Legendre polynomial and how this shows up in the Dalitz plot in figure 2.8 a) in the spin 2 state. The amplitude is manipulated in a way such that the density of events is narrow at an invariant mass and the effect of the Legendre polynomial is shown. The plots on top and to the right of figure 2.8 a) represents the projection onto  $s_2$  and  $s_1$  respectively. Figure 2.8 b) shows the Legendre polynomials of order 0,1,2,3. The odd-numbered spin states are dashed. For an example of the spin 0 and spin 1 case see figure 3.1 and figure 3.2 respectively.

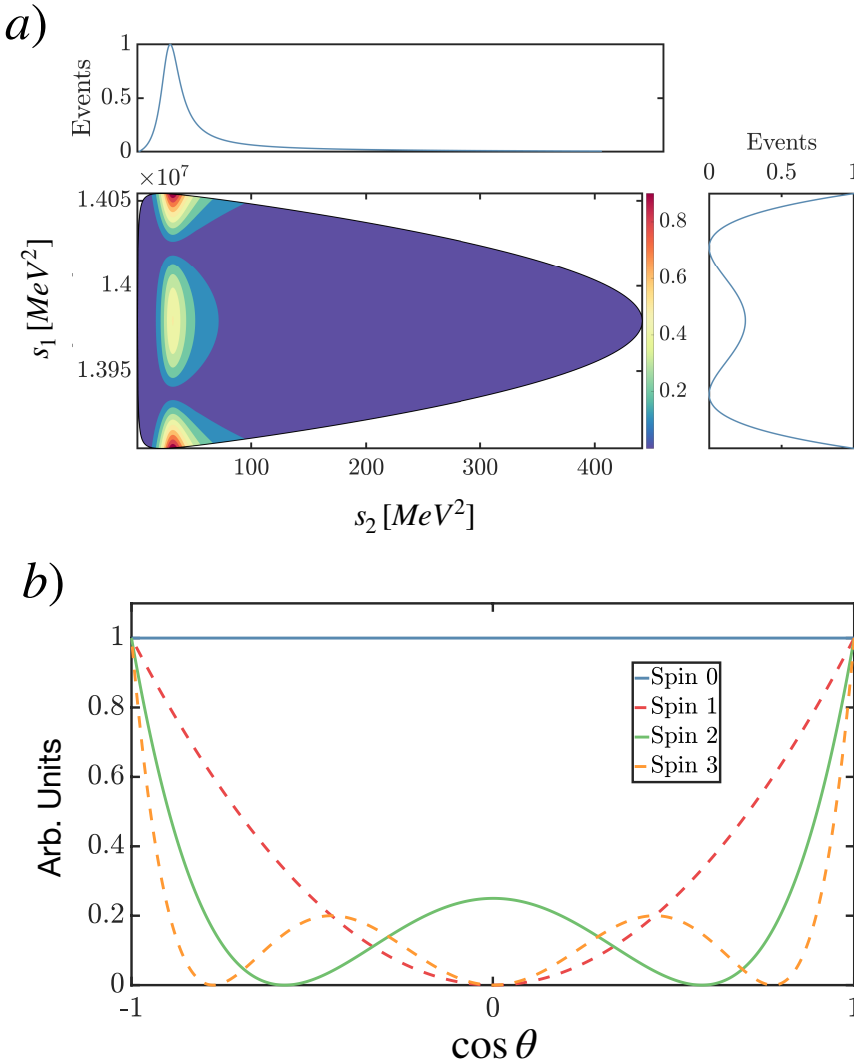


Figure 2.8: Plot illustrating the effects of the Legendre polynomials due to the spin state of a resonant particle. a) is the spin 2 state b) is the Legendre polynomial for different spin states. The odd-numbered spin states are dashed.

The projection onto the axis  $s_2$  and  $s_1$  have been calculated using equation (2.59) and (2.60) and these have been plotted as a function of an invariant mass.

To summarize, I have presented the Dalitz formalism. I introduced the kinematics of decays with three particles in the final state and explained the boundary curve using equation (2.46). Hereupon I advocated the non-uniformity of events within the boundary curve using the relativistic expression of the Breit-Wigner equation (2.59) combined with equation (2.60). I have tried to keep all the expressions as general as possible yet justifying the equations with examples of specific decays. I have done it this way to pave the way for a specific particle, the hypothetical X17 particle.

### 3 X17

---

In the following, I will present the results of using the formalism described in section 2 concerning the X17 particle hypothesised to explain anomalous measurement results. The introduction to the X17 particle is described in section 1. I will combine the theory from section 2 with the experimental results from the helium experiment in which a peak in electron-positron angular correlation was observed at  $115^\circ$  with  $7.2\sigma$  significance.

To outline why the angular correlation yields evidence of the X boson I will be stating without proof that the relation between the scattering angle  $\theta_C$  in the CMS and the angle in the laboratory system for two-particle scattering is given by

$$\tan \theta_C = \frac{1}{\gamma} \frac{q' \sin \theta_C}{q' \cos \theta_C + v E'}, \quad E' = m_P \gamma \quad \text{and} \quad q' = m_P u \gamma. \quad (3.1)$$

where  $m_P$  is the mass of the projectile and  $u$  is the magnitude of the velocity of  $P$  in the centre of mass frame [Martin and Shaw 2019, 460]. Introducing a few approximations yields that unless  $u \sim c$  and  $\cos \theta_C \sim -1$  the final state particles will be placed in a narrow cone parallel to the beam direction. In the case of the following decay  ${}^4\text{He}^* \rightarrow {}^4\text{He} + \text{X}$  the decay products were not placed in a narrow cone hence the anomaly. This means the analysis of the angular correlation between the electron-positron pair is of great interest and can be investigated using the formalism in section 2 since this makes an explicit expression for the angle between the particles in a three-particle decay for different spin states of a resonant state. For this reason, I have split the following sections into three for the three different spin states of the resonant particle.

The figures in this section are created using equations from section 2 but I have modified some of the values for visual and pedagogical purposes. Specifically, I have changed  $\Gamma$  to 2 MeV in equation (2.56) on all figures. The figures are identical but only the spin states are changed according to equation (2.61).

The figures also include different values for the mass of the X boson. These modifications are represented as dashed lines in the projection onto  $s_2$ . These show how a decreasing mass of the X boson yields a lesser value of the invariant mass  $s_2$ . As a sanity check, this can be compared to the figure representing the kinematical regions of the Dalitz plot 2.5<sup>1</sup>. The maximum value of  $s_2$  represents an angular separation of  $\pi$  radians between the electron-positron pair. The minimum of  $s_2$  is when the electron-positron pair is parallel and this is the case when  $m \approx 1/3m_X$ . This is the red dashed line in figure 3.1.

The scenario of maximum is also illustrated in the figure. This is the green dashed line that represents the maximum of  $s_2$  which occurs when  $m \approx 1.2m_X$ . The exact values for minimum and maximum of  $s_2$  can be calculated using equation (2.53) but I have chosen slightly different values to show the behaviour of the entire curve. As the mass of the X boson approaches the mass of the photon the angular separation between the electron-positron pair approaches 0 which is consistent with equation (3.1) and figure 2.5.

The resonance band is perpendicular to the  $s_2$  axis since the final state products are  $\text{He}(e^- e^+)$ , where the parenthesis represents the decay channel of the resonant state cf. section 2.4. The width of the resonance band is not a representation of the values in the experiment since I have changed  $\Gamma$ .

The projection onto the  $s_1$  axis is identical for all figures and the Breit-Wigner equation has a peak at  $s_2 = 278.89 \text{ MeV}^2$ . I calculated the exact value of  $s_2$  from the peak of the Breit-Wigner equation at  $m_X^2 = 278.89 \text{ MeV}^2$ .

Finally, I will make the approximation that the CMS is comparable to the laboratory system since  $m_1 \gg m_2, m_3$ . I would like to empathize that this is my original way of representing the projection onto the respective axis.

---

<sup>1</sup>I have swapped the axis

### 3.1 Spin 0

Figure 3.1 is made by using equation (2.46) for the kinematically restricted phase space and equation (2.62) for the resonant behavior. In figure 3.1 I have also included a dashed line inside the Dalitz plot which shows how the experimental values would be represented. I have used equation (2.45) with  $\cos(115^\circ)$ .

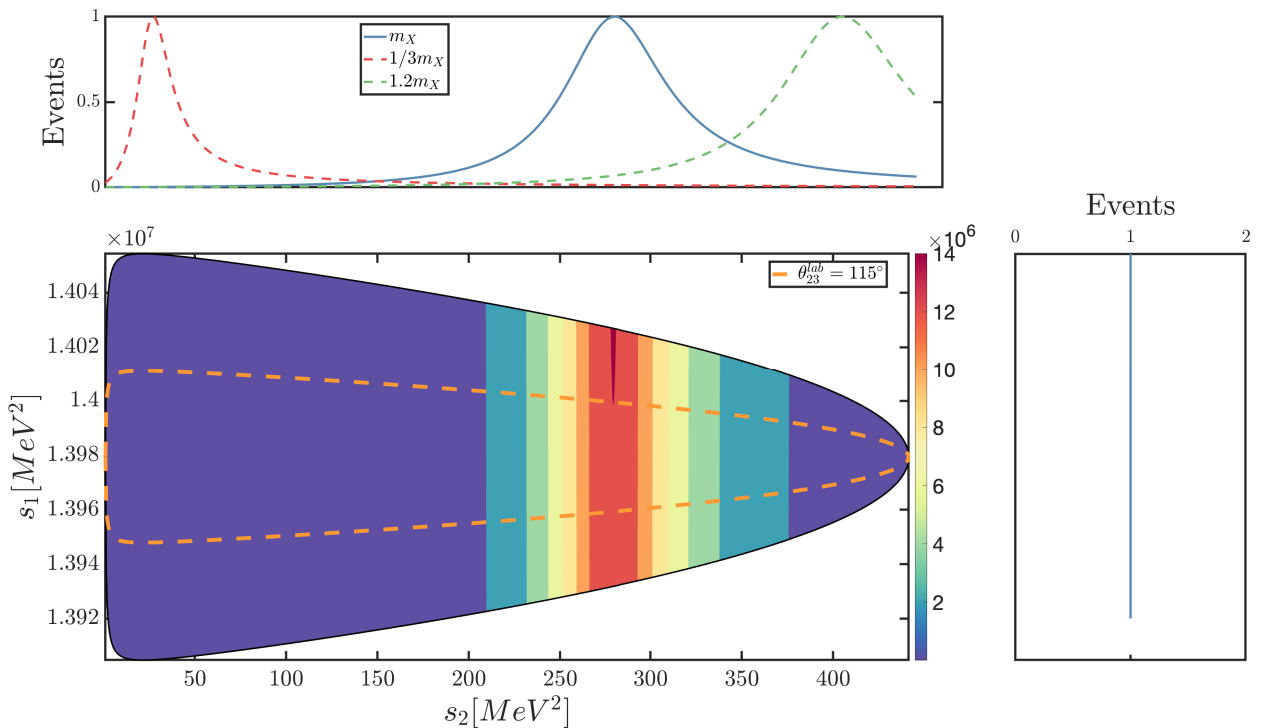


Figure 3.1: Dalitz plot of the decay  ${}^4\text{He}^* \rightarrow {}^4\text{He} + e^+ + e^-$  with a resonant state consisting of the hypothetical X boson in the spin 1 state. The angular distribution is constant and this is shown in the projection onto the  $s_1$  axis. The resonance band is perpendicular to the  $s_2$  axis since the final state products are  $\text{He}(e^- e^+)$ .

### 3.2 Spin 1

Considering the scenario where the spin state of the X boson is 1. From equation (2.61) I would expect the intensity in the middle of the Dalitz plot to be zero correspondings to  $\cos \theta_{12} = 0$ . This is shown in figure 3.2. The angular distribution along  $s_1$  is given by a Legendre polynomial of order 1.

In other words, the resonance in figure 3.2 is characterized by the relativistic Breit-Wigner shape and the angular dependence of the decay angles.

There are several interesting regions on figure 3.2 but I will focus on the minimum value of the projection onto  $s_1$ . This point in the Dalitz plot is exactly the case where  $\cos \theta_{12}^{\text{CMS}} = 0$ . In section 2 I derived an expression for the angle between particle 1 and particle 2 in the rest frame of particle 2 and 3. This is equation (2.47) and an analogous equation for the angle between the particles 1 and 2 can be found in the CMS. Plugging the numbers into this equation gives  $\theta_{23}^{\text{CMS}} = 105.3^\circ$  and this should be considered an experimental prediction.

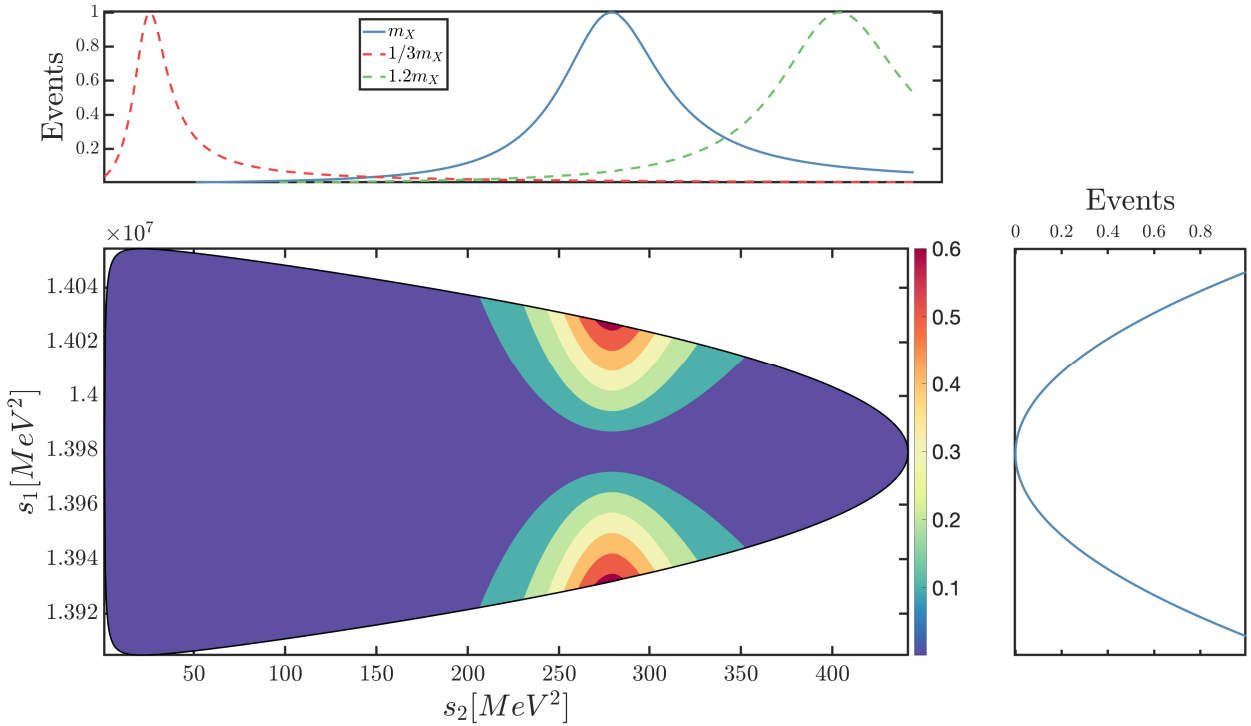


Figure 3.2: Dalitz plot of the decay  ${}^4\text{He}^* \rightarrow {}^4\text{He} + e^+ + e^-$  with a resonance state consisting of the hypothetical X boson in the spin 1 state. The angular distribution is given by  $\cos \theta$  and this is shown in the projection onto the  $s_1$  axis. The resonance band is perpendicular to the  $s_2$  axis since the final state products are  $\text{He}(e^- e^+)$ .

As a sanity check I know the centre of the Dalitz plot corresponds to  $s_2 = 220 \text{ MeV}^2$  should have  $\cos \theta_{23}^{\text{CMS}} = 0$  since the entire boundary curve is defined by  $\cos \theta = 1$  in the lower end and  $\cos \theta = -1$  at the higher end. I

then calculate  $\cos \theta_{23}^{\text{CMS}}(s_2 = 220) = 89.8^\circ$  which is approximately the centre of the plot. Also since  $s_2(m_X^2) > s_2(220)$  the cosine of the angle to  $m_X^2$  should be between 0 and -1 which is consistent with  $\cos(105^\circ) \approx -0.26$ . This analytical approach can be used for any point on the Dalitz plot and for all  $\theta_{ij}^{\text{CMS}}$  since  $s_3$  is constrained from equation (2.35).

### 3.3 Spin 2

Considering the spin 2 case I expect two regions with zero events due to the  $P_2$  term in equation (2.59). From figure 2.8 b) this resembles a Mexican hat curve. The result is shown in figure 3.3. The maximum intensity of events is in the centre of the Dalitz plot. This might seem odd at first considering the projection onto the  $s_1$  axis. One might expect the maximum intensity of events near the boundary curve, but this region is restricted due to conservation of momentum.

This also means that the intensity of events would be greater if the mass of the X-boson was  $1/3 m_X$  illustrated by the dashed red line. This would shift the Breit-Wigner peak towards lower values of  $s_2$  and would result in a greater intensity near the boundary curve. This is illustrated in figure 2.8 a). I interpret the intensity of events as a probability density function and this shows how the kinematics of the decay restricts the probability of a specific angular configuration – since different regions in the Dalitz plot represent different momenta configurations.

I will consider the two lines parallel to  $s_2$  with zero intensity. These lines represent  $\frac{1}{2}(3 \cos^2 \theta - 1) = 0$  in equation (2.62). To get more information about the angle between the particles inside the Dalitz plot it is also possible to use the kinematical configurations in figure 2.5. Interpolating between the six points on figure 2.5 traces how the CMS momentum configuration along the boundary curve. To do this for any point inside the Dalitz plot, I would assume it to be sufficient to relax the condition  $\cos \theta_{ij} = \pm 1$ ,  $i, j = 1, 2, 3$  thus get an expression for the angle between the particles from equation (2.47) in the CMS. In figure 3.3 I have included an orange dashed line to show  $\theta_{12}^{\text{CMS}} = 25^\circ$ . These lines are not uniquely defined since the boundary curve from equation (2.46) consists of an upper and lower half and adding  $\pi$  radians corresponds to swapping the two halves of the boundary curve. The predicted angles are therefore  $\theta_{12}^{\text{CMS}} = 25^\circ$  and  $\theta_{12}^{\text{CMS}} = 205^\circ$ .

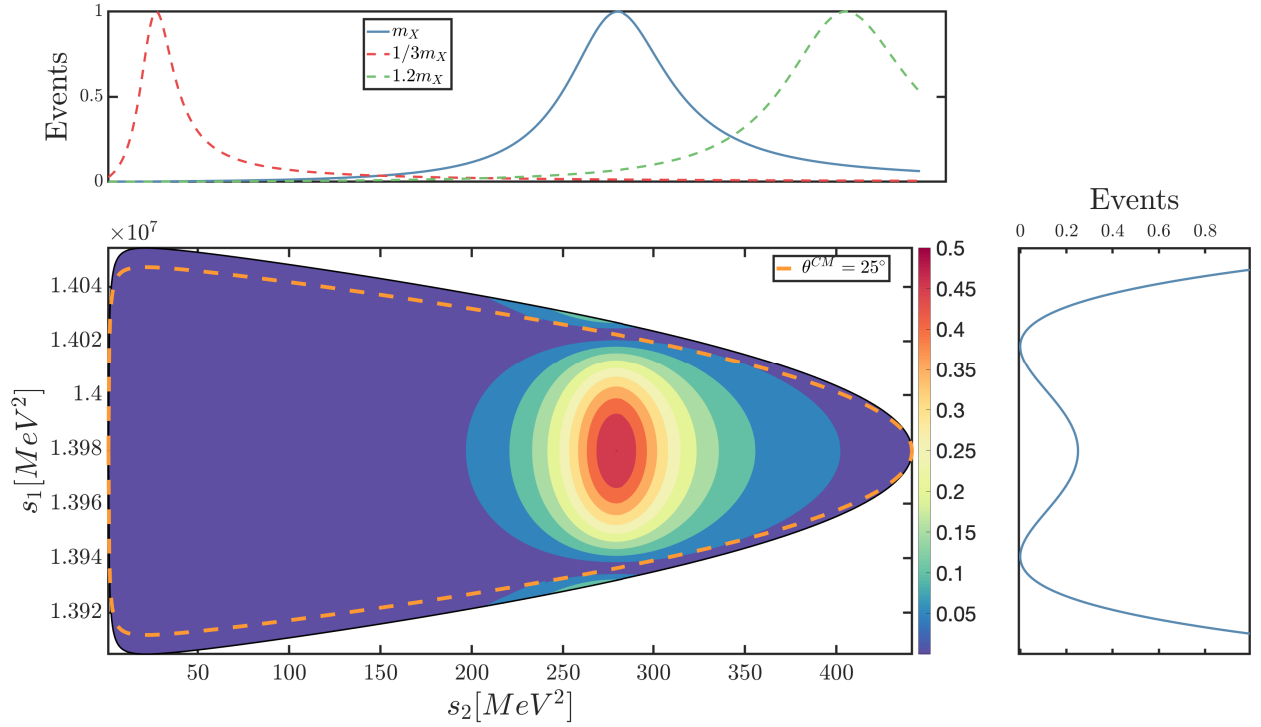


Figure 3.3: Illustration of the  ${}^4\text{He}^* \rightarrow {}^4\text{He} + e^+ + e^-$  decay with the boundary curve and resonance of the X boson in the spin 2 state. The angular distribution is given by  $\frac{1}{2}(3 \cos^2 \theta - 1)$  and this is shown in the projection onto the  $s_1$  axis.

## 4 Discussion

---

I wish to discuss the strengths and weaknesses of the Dalitz formalism. Generally speaking, moving from a two-body problem to a three-body problem is non-trivial but in the case of particle decay, the Dalitz formalism yields an elegant way of visualising the phase space. Even though I have not covered this, analysis of the amplitude yields information on the relative phases between states and can also determine CP-violating phases. In the relativistic limit, the Dalitz plot formalism is an excellent tool for visualising decays in nuclear states and the formalism is not only restricted to particle spectroscopy. In the decay I have considered the formalism is limited, in the sense that it is difficult to calculate the scattering angle for a three-body decay in the laboratory system. I introduced the approximation that the CMS is almost equal to the laboratory system but a better approach would be to boost to the laboratory system. Especially when trying to detect such small energies with high precision. Ultimately how useful this formalism is to describe the angular distributions depend on experimental confirmation.

For the X17 boson, independent confirmation is needed. There are several experiments looking for a so-called "Dark Photon". The PADME experiment (Positron Annihilation into Dark Matter Experiment) at Laboratori Nazionali di Frascati of INFN aims to search for a "Dark Photon" using positron on target collision at the DAΦNE Beam Test Facility. If the X17 particle is the Dark Photon PADME should be able to detect it since its mass sensitivity is between 1 and 22 MeV.

This is related to the results I presented in section 2.4 since the search for the X17 boson could be narrowed down if the proton beam could produce the X17 in resonance, that is  $278.89 \text{ MeV}^2$  which is the location of the Breit-Wigner peak on the  $s_2$  axis. This would increase the number of X17 particles and hence increase the probability of detection.

## 5 Conclusion

---

In this project, I have illuminated three-particle decays through kinematic invariants. In section 2, I briefly covered 2-particle scattering which leads to 3-particle decays with a focus on the boundary curve of the graphical representation of the phase space. I assigned momentum configurations to the different regions and illuminated how resonances manifest themselves in this plot. This ultimately leads to theoretical considerations of hypothetical X17 particle and I show how the formalism is consistent with relativistic scattering processes in the laboratory system and how experimental results can be represented. I also propose three angles to measure experimentally to investigate the X17 particle further.

# Bibliography

---

- Byckling, E. and Kajantie, K. (1973). *Particle Kinematics*. John Wiley & Sons, 1973 edition.
- Feng, J. L., Fornal, B., Galon, I., Gardner, S., Smolinsky, J., Tait, T. M. P., and Tanedo, P. (2016). Protophobic Fifth-Force Interpretation of the Observed Anomaly in  ${}^8\text{Be}$  Nuclear Transitions. *Phys. Rev. Lett.*, 117(7):071803.
- Feng, J. L., Fornal, B., Galon, I., Gardner, S., Smolinsky, J., Tait, T. M. P., and Tanedo, P. (2017). Particle Physics Models for the 17 MeV Anomaly in beryllium Nuclear Decays. *Phys. Rev. D*, 95(3):035017.
- Goetzen, K. (2014). Root based tool to plot 3-body decays with resonant behaviour. <https://github.com/KlausGoetzen/DalitzGUI>.
- Hagedorn, R. (1963). *Relativistic Kinematics*. W.A. Benjamin, inc., 1964 edition.
- Jackson, J. D. (1999). *Classical Electrodynamics*. Wiley, third edition edition.
- Kitahara, T. and Yamamoto, Y. (2017). Protophobic light vector boson as a mediator to the dark sector. *Phys. Rev. D* 95, 015008 (2017).
- Krasznahorkay, A. et al. (2016). Observation of anomalous internal pair creation in Be8 : A possible indication of a light, neutral boson. *Phys. Rev. Lett.*, 116(4):042501.
- Krasznahorkay, A. et al. (2019). New evidence supporting the existence of the hypothetic X17 particle.
- Lancaster, T. and Blundell, S. J. (2014). *Quantum Field Theory for the Gifted Amateur*. Oxford University Press, first edition.
- Londergan, T. (2015). Geometrical methods for data analysis i: Dalitz plots and their uses.

Martin, B. R. and Shaw, G. (2019). *Nuclear and Particle Physics: An Introduction*. Wiley, 3rd edition.

Taylor, J. R. (1972). *Scattering Theory. The Quantum Theory of Nonrelativistic Collisions*. Dover, 2006 edition.

Uggerhøj, U. I. (2016). *Speciel Relativitetsteori*. Aarhus Universitetsforlag, 1st edition.

Zyla and others (Particle Data Group) (2020). to be published in *prog. theor. exp. phys.*

# A

---

In this project, I have described an approach to analysing the hypothetical X17 boson. In this appendix, I will outline the problems the X17 boson could solve. This will include the  $(g - 2)_\mu$  anomaly and also why the X17 is a candidate for dark matter hence the crossover with cosmology mentioned in the preface. This appendix will review some of the possibilities and I will show the equations without proof. For a thorough description see [Feng et al. 2016]. A priori the X boson may be a scalar, pseudoscalar, vector or even a spin-2 particle. I will outline the reasoning of Feng et al. as to why they can exclude the different types of particle candidates and focus on the vector boson case.

The scalar particle candidate can be excluded due to conservation of parity in the transition  ${}^8\text{Be}^* \rightarrow {}^8\text{Be} + \text{X}$ .

Pseudoscalar and axion-like candidates can be excluded since couplings to the photons for a 17 MeV particle are experimentally excluded. This atleast outlines the considerations the group made. For a full explaination see [Feng et al. 2017, 7-9]. If one supposes a vectorlike interaction between the Standard Model matter fields and the light vector boson, the consistency in the other experimental results requires that the interaction should be protophobic. The coupling to the up and down quark and the electron are given by [Feng et al. 2016; Kitahara and Yamamoto 2017]

$$2.0 \cdot 10^{-4} \lesssim |g_u| \lesssim 1.0 \cdot 10^{-3} \quad (\text{A.1})$$

$$4.0 \cdot 10^{-4} \lesssim |g_d| \lesssim 2.0 \cdot 10^{-3} \quad (\text{A.2})$$

$$6.1 \cdot 10^{-5} \lesssim |g_e| \lesssim 4.2 \cdot 10^{-4}. \quad (\text{A.3})$$

This means the coupling to the proton ( $2g_u + g_d$ ), neutron ( $g_u + 2g_d$ ) and the electron can be calculated. Surprisingly the X17 boson couples more strongly to the neutron than the proton. In other words this means that in order to explain the anomaly measured in the Beryllium experiment Feng et al. are proposing a protophobic boson. This gauge boson couples non-chirally to

Standard Model fermions with charged  $\varepsilon_f$  in units of  $e$ . They impose several constraints and end up with

$$\varepsilon_u = -\frac{1}{3}\varepsilon_n \approx \pm 3.7 \cdot 10^{-3}, \quad (\text{A.4})$$

$$\varepsilon_d = \frac{2}{3}\varepsilon_n \approx \mp 7.4 \cdot 10^{-3}, \quad (\text{A.5})$$

$$2 \cdot 10^{-4} \lesssim |\varepsilon_e| \lesssim 1.4 \cdot 10^{-3}, \quad (\text{A.6})$$

$$|\varepsilon_\nu \varepsilon_e|^{1/2} \lesssim 7 \cdot 10^{-5}. \quad (\text{A.7})$$

For  $|\varepsilon_e|$  near the upper limit and  $|\varepsilon_\nu| \approx |\varepsilon_e|$  the X boson also solves the  $(g - 2)_\mu$  problem, reducing the discrepancy to below  $2\sigma$  [Feng et al. 2016, 4]. This problem originates from the Dirac equation which predicts  $g = 2$  for particles such as the electron. The result of this factor differs from the measured value and the difference is called the anomalous magnetic moment given by

$$a = \frac{g - 2}{2} \quad (\text{A.8})$$

In the case of the muon this is the problem the X17 boson explains. An experiment at Fermilab named *Muon g - 2* will improve the accuracy on this magnetic dipole moment for the muon.

To explain how the X17 is related to dark matter one can use the protophobic property of this particle and  $\Gamma_X = 3.9 \cdot 10^{-5}$  eV. This means that a particle with a mass of 17 MeV decays almost before one can observe it and it interacts weakly with matter. The protophobic property means that it does not interact significantly with almost all the matter the universe is made of. This is why the X17 boson is a candidate for dark matter.